Journal of Sedimentary Research

Journal of Sedimentary Research, 2021, v. 91, 349–361
Research Article
DOI: 10.2110/jsr.2021.01

LIPID COMPOSITION OF THE MICROBIAL MAT FROM A HYPERSALINE ENVIRONMENT (VERMELHA LAGOON, RIO DE JANEIRO, BRAZIL)

TAIS FREITAS DA SILVA,[1] SINDA BEATRIZ CARVALHAL GOMES,[2] FREDERICO SOBRINHO DA SILVA,[3] KSENIJA STOJANOVIĆ,[3] ROSANE NORA CASTRO,[4] JOÃO GRACIANO MENDONÇA FILHO,[2] AND MILTON SANTOS[2]

[1]*Department of Geology, Institute of Geosciences, Federal University of Rio Grande do Sul, Avenida Bento Gonçalves 9500, Prédio 43126 Sala 201, CEP 91509-900 Porto Alegre, Brazil*

[2]*Department of Geology, Institute of Geosciences, Federal University of Rio de Janeiro, Avenida Athos da Silveira 274, Prédio do CCMN, Sala J1020, Campus Ilha do Fundão, CEP 21949-900 Rio de Janeiro, RJ, Brazil*

[3]*University of Belgrade, Faculty of Chemistry, Studentskitrg 12-16, 11000 Belgrade, Serbia*

[4]*Institute of Chemistry, Federal Rural University of Rio de Janeiro, Rio de Janeiro, CEP 23897-000 Seropédica, Brazil*

e-mail: tais.freitas@ufrgs.br

ABSTRACT: **This study determines organic-matter (OM) composition in the different color layers of a stratified hypersaline microbial mat and verifies the hypothesis that each layer includes a distinct group of lipids. The relation of precursor lipids from the microbial mat to the hydrocarbon composition in fossil records was also evaluated. To that end, the composition was studied of glycolipids (GLs), phospholipids (PLs), and "neutral" lipids (NLs, including hydrocarbons, *n*-alkanols, sterols, hopanols, free fatty acids, and wax esters) in four different color layers (A–D; depth intervals: up to 0.5 cm, 0.5–1.0 cm, 1.5–3.0 cm, and 3.0–6.0 cm, respectively) of a stratified hypersaline mat from the Vermelha Lagoon, Rio de Janeiro, Brazil.**

Microscopic characterization revealed the presence of 16 cyanobacterial morphospecies, with predominance of *Microcoleus chthonoplastes*. The notable prevalence of saturated straight-chain fatty acids (FAs), *n*-16:0 and *n*-18:0 and their monounsaturated counterparts, *n*-16:1 and *n*-18:1 in all three lipid fractions (GLs, PLs, and NLs), associated with the domination of *n*-C_{17} alkane and *n*-$C_{17:1}$ alkene among the hydrocarbons confirmed the main imprint of cyanobacteria. The composition of the studied lipid classes implies the contribution of sulfate-reducing bacteria such as *Desulfomicrobium* sp. strain, purple sulfur bacteria, as well as the possible input of *Geobacter* spp. and *Desulfovibrio* spp., particularly in the deeper layers.

The notable decrease in total extractable lipids (TELs) yield from layers A to D indicates that lipid synthesis is far more intense by photosynthesizing cyanobacteria than by anaerobic microorganisms. The content of PLs was uniform and low (< 5%) in all layers, implying their extremely quick degradation. GLs, followed by NLs, were the most abundant in all layers indicating the medium, which is characterized by carbon source excess and limited nitrogen source, which regulates microorganism growth. The upper layers, A (green) and B (reddish-brown) differ from those lower, C (dark brown greenish) and D (brown) according to the NLs/GLs ratio, which is higher in the former.

The lipid compositions reveal distinctions between the individual layers in the microbial mat. The observed layers clearly differ according to the amount of high-molecular-weight (C_{22}–C_{31}) *n*-alkanes and long-chain (C_{21}–C_{30}) *n*-alkanols, the content of phytol, bishomohopanol, tetrahymanol, C_{27}–C_{29} sterols, the stanol/stenol ratio in the neutral lipid fraction, as well as the content of branched (*iso* and *anteiso*) FAs and w9/w7 FA ratio in the GLs fraction. The mentioned parameters imply a greater contribution of sulfate-reducing and purple sulfur bacteria to layer B, higher impact of photosynthetic red algae in upper layers A and B, the elevated contribution of marine ciliate species, feeding on bacteria to layers B and C, as well as the increment of anoxygenic phototrophic and heterotrophic bacteria to layer D. The greatest capability for the synthesis of hydrocarbons is observed in layer B.

The composition of lipid classes in the microbial mat showed a significant relationship with the most important biomarkers' fingerprints in the source rocks extracts and petroleum derived from the carbonate hypersaline environments, including the distribution of *n*-alkanes, a high abundance of phytane and gammacerane, as well as a distribution of C_{27}–C_{29} regular steranes. Therefore, these results offer an insight into the transformation of microbial OM during the sedimentation processes in a hypersaline environment and its contribution to the fossil record.

Published Online: April 2021
 1527-1404/21/091-349

INTRODUCTION

Lipid biomarkers are a powerful tool to characterize the microbial community structure in microbialites (Kaur et al. 2011). For example, archaeal and bacterial lipid distributions and carbon isotopic composition have proved effective to characterize mat-building organisms in geothermal systems, and microbial communities in cold-seep carbonates.

Microbial mats are laminated biofilms that grow mostly on submerged or moist surfaces. They usually develop in heat- and/or salinity-stressed habitats, and the organisms are often spatially organized as a result of physicochemical gradients (Pierson et al. 1994; Rontani and Volkman 2005; Sánchez et al. 2006). They are generally composed of a few groups of microbes: cyanobacteria, colorless sulfur bacteria, purple sulfur bacteria, and sulfate-reducing bacteria (Boudou et al. 1986; Dobson et al. 1988; van Gemerden 1993). The lower diversity of species in these ecosystems provides a qualitative differentiation of the sources of autochthonous (bacterial, algal, and macrophytes) from the allochthonous organic matter (OM) in sediments and the recognition of early diagenetic processes, which can be used for biogeochemical modeling studies (Grimalt et al. 1992).

In mats, bacterial activities involve complex syntrophic communities in which the photosynthesis in the upper mat is balanced by decomposition below (Grimalt et al. 1992). The result is a well-defined stratified benthic community with aerobic phototrophs (cyanobacteria) in the near surface, anoxygenic phototrophs below, followed by chemoorganotrophs that require neither oxygen nor light (Riding 2000). Therefore, their individual layers tend to be populated by specific organisms (e.g., cyanobacteria, purple photosynthetic bacteria, sulfate-reducing bacteria) which facilitates the differences in the OM of various mat horizons to be assessed in terms of the contributions from, and effects of, these different microorganism (Boudou et al. 1986).

Since modern microbial mats are considered analogues for ancient sediments, the bacterial activities have been studied using lipids, which are biomolecules that have a great preservation potential and therefore are readily preserved over geological timescales (Riding 2000; Plet et al. 2018). Lipid analysis has been used to identify specific microbial groups from a variety of localities and environmental settings (Navarrete et al. 2000; Bühring et al. 2009; Allen et al. 2010; Pagès et al. 2014; Plet et al. 2018).

In lipid studies, three subdivisions are recognized: "neutral" lipids (NLs), glycolipids (GLs), and phospholipids (PLs) (Kates 1972). The "neutral" lipids include aliphatic hydrocarbons, wax esters, free fatty acids, free sterols, and free alcohols. The wax esters and free fatty acids (FAs) are common storage lipids in protozoa and eukaryotic algae (Piorreck and Pohl 1984), whilst the free sterols are ubiquitous in all organisms other than bacteria. GLs are sugar-containing lipids which are more polar than the PLs and are abundant constituents of many gram-positive bacteria and some gram-negative bacteria. However, algae and higher plants also produce GLs (Lechevalier and Moss 1977). On the other hand, PLs are the membrane constituents of all organisms (Gillan and Sandstrom 1985).

These characteristics prompt a focus on the distribution and composition of NLs (free FAs, hydrocarbons, *n*-alkanols, sterols, hopanols, wax esters) and methyl esters of FAs obtained by methanolysis of GLs and PLs in the microbial mat from the hypersaline Vermelha Lagoon, Rio de Janeiro, Brazil, which could improve the interpretation of biosignatures in pre-salt petroleum reservoirs.

Although several researchers have studied this lagoon with a focus on geology, biology, taxonomy, and geochemistry (Knoppers and Kjerfve 1999; van Lith et al. 2002; Silva E Silva et al. 2004, 2005; Silva and Carvalhal 2005; Damazio and Silva E Silva 2006; Laut et al. 2017; Ramos et al. 2017; Rocha and Borgui 2017), this article probably represents one of the first reports to determine and quantify polar lipid composition, and test the capability of these biomolecules to distinguish individual layers in a microbial mat. Furthermore, it is well known that the source rock kerogen, which is a heterogeneous, polymeric material formed from a biomass consisting of variable proportions of algae, higher plants, and bacteria remains (Tissot and Welte 1984), represents the main precursor of petroleum via geothermal maturation. The contribution of algae and higher plants to sedimentary OM is well documented using microscopic techniques (e.g., maceral composition) and biomarker patterns (*n*-alkanes, steroids, gymnosperm-derived diterpenoids, angiosperm-derived non-hopanoid triterpenoids, botryococcane, polymethylsqualanes; Peters et al. 2005), whereas evidence of the contribution from bacteria is usually referred to the presence of hopanoids (Nytoft 2011). Therefore, the second study objective was to connect the composition of precursor lipids in the microbial mats with the composition of ancient biomarkers commonly present in source-rock extracts and petroleum, which provides the essential data to better understand the transformation of microbial OM during sedimentation processes and its contribution to the fossil record.

MATERIAL AND METHODS

Study Area

The Vermelha Lagoon (Lagoa Vermelha) is a shallow, hypersaline, and carbonaceous coastal lagoon on the southeast coast of Rio de Janeiro State, Brazil. It is approximately 4.5 km long and 250 to 850 m wide, covering an area of 1.90 km^2 with a mean water depth of 2.0 m. The Vermelha lagoon is situated between two parallel dune systems, the younger (Holocene), which separates it from the Atlantic Ocean, and the older (Pleistocene), which separates it from the much larger lagoon, Araruama Lagoon (Fig. 1) (van Lith et al. 2002).

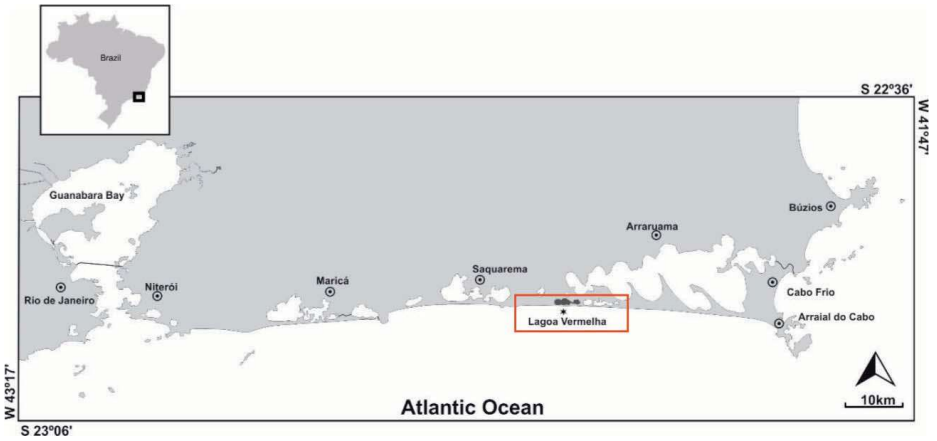

FIG. 1.—Map showing the location of Lagoa Vermelha on the southeastern coast of the state of Rio de Janeiro, Brazil.

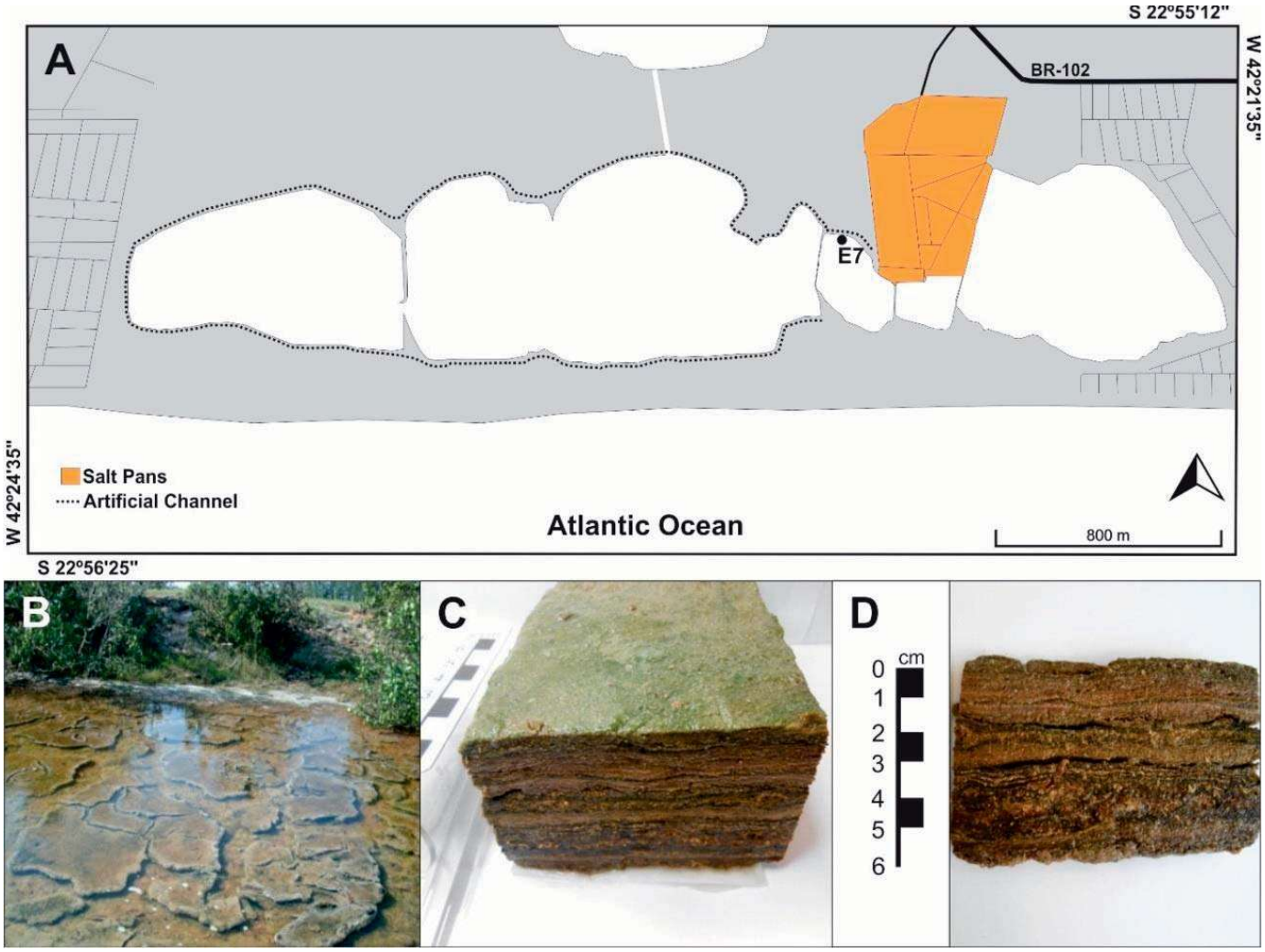

FIG. 2.—Sampling location at the Vermelha Lagoon. **A)** Detail map of Lagoa Vermelha showing the E7 sampling site. **B)** Photo of polygonal mat collected at E7 site. **C**, **D)** Transversal cut showing inner laminae and color zonation of the microbial mat collected.

There is no surface drainage into the lagoon environment, hence the water balance is controlled by weather conditions (dry or rainy season). The underground inflow of ground waters and sea conditions promote seepage, which can considerably increase the lagoon's water volume. The water body is fragmented into five interconnected ponds with different dimensions arising from decades of salt explorations (Knoppers and Kjerfve 1999).

The high salinity, sulfate-reducing bacterial activity, indicated by the presence of sulfide and positive $\delta^{34}S$ of sulfate, and biotic or abiotic sulfide oxidation are the main controls on dolomite formation in sediments (van Lith et al. 2002; Moreira et al. 2004). This special mineralogical composition of sediments is in contrast with the neighboring lagoons, where detrital sedimentation predominates (Vasconcelos et al. 2006).

Living microbial mats and stromatolites have been described for the Vermelha Lagoon in areas that are flooded periodically or intermittently, such as intertidal or adjacent supratidal environments like temporary pools (Silva E Silva et al. 2004; Silva E Silva and Carvalhal 2005).

Sampling

The mat sample was collected from a small central Vermelha Lagoon pond which borders saltpans (Fig. 2). The mat was classified in morphotype, according to its geometry, texture, and color at the sampling site. The sample was collected using a metal spatula, placed into an aluminum container, and refrigerated during transport.

The sample was characterized regarding cohesion, inner lamination, and color zonation by stereoscopic microscopy, and then cut into four parts according to color and freeze-dried for lipid analyses. For cyanobacterial analyses, the mat was preserved in a formaldehyde solution (4%).

Identification of Cyanobacteria

Emphasis was placed on the cyanobacterial taxa, which are key organisms and which dominate the mat biomass (Dijkman et al. 2010). Approximately ten slides from the mat were microscopically observed (Axiovision Imager.A1 Zeiss) to ensure a good overall representation of resident morphotypes. The taxonomic identification was carried out in accordance with traditional morphological features.

Lipid Analysis

The layers of mat were extracted with a solvent mixture dichloromethane/methanol (2:1, v/v) using an accelerator solvent extractor (ASE). The extracts were fractionated using benzenesulfonic acid bonding solid-phase

extraction (SPE) columns (DSC-SCX; 500 mg, 3 cm^3). The fractions were eluted sequentially with dichloromethane, acetone, and methanol to obtain neutral lipids, glycolipids, and phospholipids fractions, respectively. The neutral lipids were fractionated using column chromatography (5 g silica-gel 70–230 mesh (63–200 μm), pore size 60A°, dried at 110 °C for 8 h) and five fractions were eluted with 10 cm^3 *n*-hexane, 9 cm^3 *n*-hexane/dichloromethane, 10 cm^3 dichloromethane, 10 cm^3 dichloromethane/acetone and 15 cm^3 dichloromethane/methanol yielding, respectively: F1 containing hydrocarbons, F2 containing ketones, F3 containing esters, F4 containing sterols and alcohols, and F5 containing acidic compounds. Fractions were concentrated by rotary evaporation. After solvent evaporation, the residues of fractions F4 and F5 were taken up in 100 μl of BSTFA (Supelco) and silylated for 1 h at 50 °C.

The glycolipids and phospholipids fractions were saponified by a heating process at 100 °C in a water bath in the presence of 0.5 cm^3 of methanol/toluene (1:1, v/v) and 0.5 cm^3 of potassium hydroxide/methanol (0.2 mol/dm^3). After cooling 1.5 cm^3 of BF_3/methanol was added and the subsequent extraction performed four times with *n*-hexane. The combined *n*-hexane extracts were concentrated.

All fractions were analyzed by gas chromatography-mass spectrometry (GC-MS). The GC-MS analyses were performed using an Agilent Technologies instrument (U.S.A.) comprising a 7890A model gas chromatograph equipped with a 7693 auto sampler and coupled to a triple-quadrupole 7000B Mass Spectrometer (MS). Helium was the carrier gas, in a constant-flow mode, at 1.2 cm^3/min. A DB-1 column (100% dimethylpolysiloxane, 30 m long, with 0.25 mm inner diameter and 0.25 μm film thickness) was used. The column was heated from 40 °C (1 min, hold) to 140 °C at a rate of 20 °C/min and then to 280 °C at 2 °C/min. The final temperature of 280 °C was maintained for an additional 30 minutes. The injector and transfer line temperatures were 280 °C. The MS was operated under the following conditions: the ion source temperature was 290 °C, the interface temperature was 300 °C, and the quadrupole temperature was 150 °C. Electron impact ionization (70 eV) was used, and full scan spectra were obtained by scanning *m/z* 50–800 at 1 scan s^{-1}. The compound assignment was performed by examination and comparison with the literature mass spectra and NIST (National Institute of Standards and Technology) library. The quantitative analyses were performed by comparison of peak areas of the compounds with those of internal standards: deuterated tetracosane for hydrocarbons analysis and 5α-androstan-3β-ol for alcohols, free fatty acids, wax esters, and *fatty acid methyl esters (*FAMEs).

RESULTS

Mat Description and Cyanobacterial Diversity

External morphology of the mat sampled showed traditional features like upturned crack margins producing saucer-shaped polygons, approximately 50 cm wide and almost 6 cm thick. This mat had a flat dark pigmented green surface and internally was subdivided into four different colors layers. The top of mat showed a green layer (0.5 cm), followed by a reddish-brown layer (0.5–1.5 cm), a dark brown greenish layer (1.5–3.0 cm), and finally a thicker bottom brown layer (3.0–6.0 cm), which are assigned as A, B, C, and D, respectively. Irregular and thin carbonate laminae were observed mainly in the brown layer (D).

These color stratifications are linked to a position of different microorganism guilds in response to physiological requirements (gradients of light, oxygen, redox potential, sulfide and pH) as described by Visscher et al. (1992), Ward et al. (1998), and Stolz 2000. The positioning and morphology of the microbial mat agreed with classifications proposed for other hypersaline environments (Horodyski and Bloeser 1977; Silva E Silva et al. 2005). The occurrence of the same cyanobacterial mat in the neighboring lagoons of the Araruama system has been previously described (Silva E Silva et al. 2005; Damazio and Silva E Silva 2006; Ramos et al. 2017; Rocha and Borgui 2017).

The cyanobacteria diversity consists of sixteen morphospecies: *Aphanocapsa litoralis*, *Aphanothece marina*, *Aphanothece salina*, *Chroococcus membraninus*, *Chroococcus minor*, *Chroococcus turgidus*, *Gloeocapsopsis crepidinum*, *Gomphosphaeria aponina*, *Gomphosphaeria salina*, *Johannesbaptistia pellucida*, *Synechococcus salinarum*, *Jaaginema subtilissimun*, *Microcoleus chthonoplastes*, *Microcoleus tenerrimu*, *Phormidium okeni*, and *Spirulina subsalsa*.

Some morphospecies detected, such as *Microcoleus*, *Schizothrix*, *Spirulina*, *Aphanothece*, *Aphanocapsa*, *Chroococcus*, *Gloeocapsopsis*, *Synechococcus*, and *Johannesbaptistia*, are known for their tolerance to desiccation and elevated salinities and have been reported from hypersaline mats, lagoons, and inland evaporitic lakes (Abed and Garcia-Pichel 2001; Jonkers et al. 2003; Richert et al. 2006; Abed et al. 2008, 2015; Ramos et al. 2017). *Microcoleus chthonoplastes* was the dominant cyanobacteria in this mat and other hypersaline mats, highlighting its importance in the formation and stabilization of this mat morphology (Garcia-Pichel et al. 1996).

Total Extractable Lipids

According to the literature, in shallow aquatic environments where sunlight is available, the lipids from the uppermost layers of microbial mats represent inputs of aerobic photosynthesizing cyanobacteria and other oxygenic prototrophs while the lipids from the lower layers represent different types of anaerobic bacteria.

The yields of total extractable lipids (TELs) were 14.73, 6.84, 3.88, and 1.14 mg/g (dry mat) to layer A, B, C, and D, respectively. Glycolipids (GLs) are the major compounds present in all layers, constituting from 55.40% of TELs in the layer A to 89.30% of TELs in the layer C. The proportion of neutral lipids (NLs) of the microbial mat analyzed was 41.01%, 28.67%, 8.84%, and 17.37% of TELs in the layers A, B, C, and D, respectively. The content of phospholipids (PLs) was uniform and low ($< 5\%$) in all layers (Fig. 3).

Neutral Lipids

Compounds in the neutral-lipids (NLs) fraction include hydrocarbons, free fatty acids (FFAs), sterols, hopanols, wax esters, and alcohols (*n*-alkanols, *n*-alkenols, and alcohols with a branched isoprenoid chain) (Table 1).

Free fatty acids (FFAs) dominated in all layers, with the exception of layer D, which is characterized by a uniform concentration of FFAs and hydrocarbons (Table 1). The content of hydrocarbons is two orders of magnitude higher in layer B than in the other layers (Table 1), which may be attractive to consider for biotechnological hydrocarbon production from renewable sources, similar those from *Botryococcus braunii* (Banerjee et al. 2002). Alcohols are more abundant than sterols and hopanols in layers A and D, whereas sterols prevail over alcohols and hopanols in layers B and C. Interestingly, contents of all three compound classes show the same trend versus depth (Table 1). The hopanol concentration (C_{32} hopanol, with ββ-configuration) increases in layers B and C, which indicates changes in the bacterial community. The increase of hopanol concentration in layers B and C is associated with a rise of sterol concentration (Table 1), which suggests a higher contribution of eukaryotic organisms.

Wax esters are identified in low amounts and exhibit a decreasing trend from top to bottom, being absent in the deepest layer D (Table 1).

Hydrocarbons

n-Alkanes ranged from *n*-C_{17} to *n*-C_{35}, having a maximum at *n*-C_{17}, and were detected in concentrations of 3.95, 44.09, 0.77, and 1.57 μg/g in dry

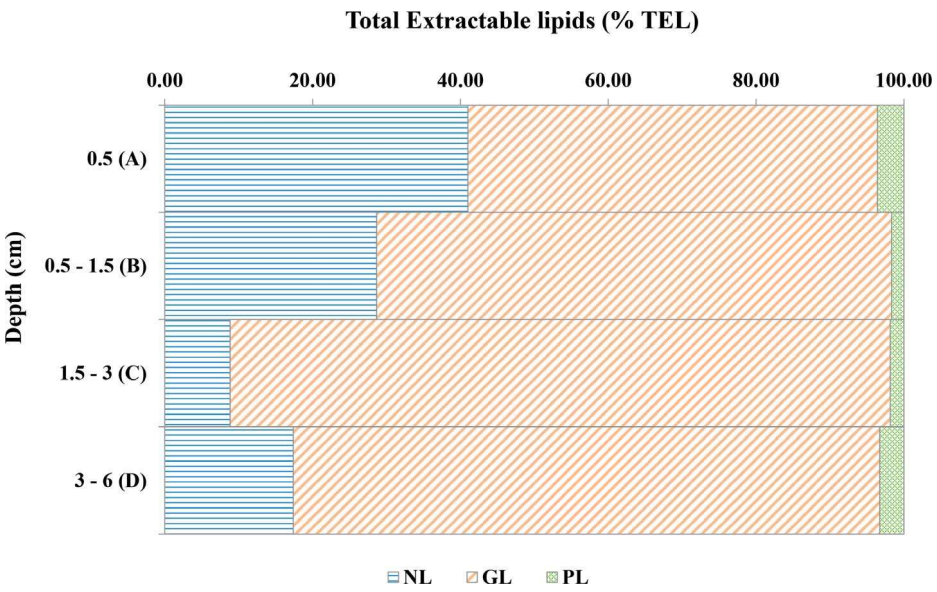

FIG. 3.—Plot of total extractable lipids (TELs) showing different composition of microbial mat layers. NLs, neutral lipids; GLs, glycolipids; PLs, phospholipids.

mat in layers from A to D, respectively. The abundance of high-molecular-weight (HMW) *n*-alkanes (> *n*-C_{21}) was the lowest at the surface (0.01 μg/g dry mat, layer A) and increased with depth to a maximum at 0.5–1.5 cm (1.53 μg/g dry mat, layer B), but decreased at 1.5–3 cm (0.19 μg/g dry mat, layer C) and increased again to 0.77 μg/g dry mat (layer D), below 3 cm.

Phytane (C_{20} regular isoprenoid) was detected in the range 0.27–17.10 μg/g dry mat, with the highest concentration in layer B and the lowest concentration in layer A. Another important isoprenoid biomarker, β-carotane, was identified exclusively in layers A and B in relatively low concentrations 0.82 and 0.54 μg/g dry mat, respectively. The absence of this biomarker in lower layers can be attributed to diagenetic alteration of the sensitive carotenoid skeleton and/or the absence of its precursors.

Pentacyclic terpenoid hydrocarbons with a hopanoid skeleton, 22,29,30-trisnorhop-17(21)-ene, 17β(H)-22,29,30-trisnorhopane, hop-17(21)-ene, and hop-22(29)-ene (diploptene) were present with total concentrations of 0.37, 0.28, 0.03, and 0.22 μg/g dry mat, in layers A to D, respectively (Fig. 4). These compounds are synthesized by a wide variety of aerobic (i.e., methanotrophs, heterotrophs, and cyanobacteria) and anaerobic bacteria, including strictly anaerobic bacteria capable of anaerobic ammonium oxidation (Rohmer et al. 1984; Volkman et al. 1986; Venkatesan 1988; Ourisson and Rohmer 1992; Summons et al. 1994; Sinninghe Damsté et al. 2004).

Free Fatty Acids

Free fatty acids (FFAs) have been used in studies of microbial mats as biomarkers for different bacterial groups, and they reflect the adaptation of bacteria to environmental stress (Grimalt et al. 1992; Abed et al. 2008; Scherf and Rullkötter 2009). Distributions of FFAs vary as a function of their source and branched short chain (C_{15} and C_{17}) are considered as "typical bacterial" free fatty acids (Rütters et al. 2002). However, long-chain fatty acids (C_{20}–C_{30}) are produced by many organisms; they may derive either directly from higher land plant material (such as cuticular waxes) or from eroded peats (Lehtonen and Ketola 1993). In addition, even-numbered long-chain fatty acids have also been discovered in some soil bacteria (Řezanka et al. 1991) and in *Desulfotomaculum* sp. (Řezanka et al. 1990).

FFAs are dominant NLs components, showing, as total lipids, a notable decrease of concentration with depth (from 1234.73 μg/g dry mat in layer A to 4.72 μg/g dry mat in layer D; Table 1). In layer A, FFAs are detected in the range C_{12}–C_{24}; layer B is characterized exclusively by the presence of short-chain (C_{12}–C_{19}) FFAs, whereas in layers C and D, FFAs are observed in the range from C_{12} to C_{30}. The ratio of short- (C_{14}–C_{20}) vs. long-chain saturated FFAs (C_{21}–C_{30}) showed the following values: 4.16 (layer C), 32.28 (layer D), 83.81 (layer A), associated with the presence of short-chain FFAs up to C_{19} only in layer B, implying a marked prevalence of the former, particularly in the upper layers. Saturated straight-chain FFAs 16:0 and 18:0 and their monounsaturated counterparts 16:1 and 18:1 dominated all layers and accounted for relative amounts from 60 to 75% of total fatty acids. The most dominant FFA was *n*-16:0, which made up ca. 31% of total fatty acids in layer A, 46% in layer B, 31% in layer C, and 52% in layer D. The amount of the fatty acid *n*-18:0 ranged between 4.13% and 18.81%, being the lowest in layer A and the highest in layer D, respectively.

TABLE 1.—*Concentrations (μg/g dry weight mat) of the isolated classes from neutral lipids fraction (quantification from GC-MS) in layers A–D.*

	Lipid Component* (μg/g dry mat)					
Layer (Depth, cm)	**Hydrocarbons**	**FFAs**	**Alcohols**	**Sterols**	**Hopanols**	**Wax Esters**
A (0.5)	7.45	1234.73	22.08	11.18	1.75	1.30
B (0.5–1.5)	144.41	229.24	25.17	26.06	6.06	1.31
C (1.5–3)	2.72	32.24	15.06	21.26	3.66	0.41
D (3.0–6.0)	4.77	4.72	0.91	0.85	0.12	N.D.

* Obtained by summing concentrations of individual components. FFAs, Free fatty acids; N.D., not detected.

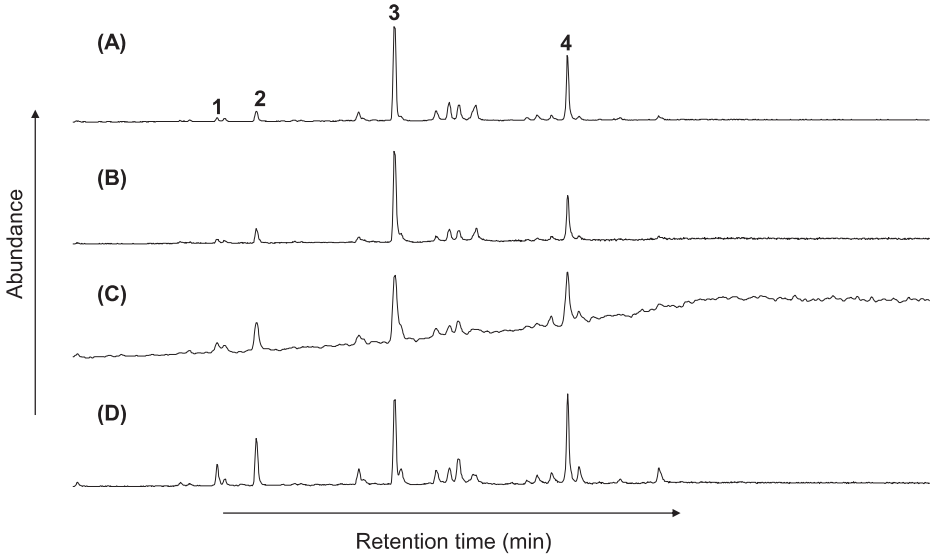

FIG. 4.—Partial mass chromatograms of *m/z* 191 showing distribution of hopanoids in the four layers of microbial mat sample. These data illustrate the predominance of four hopanes: 1) 22,29,30-trisnorhop-17(21)-ene, 2) 17β(H)-22,29,30-trisnorhopane, 3) hop-17(21)-ene, 4) hop-22(29)-ene (diploptene).

Normal, Isoprenoid, and Pentacyclic Triterpenoid Alcohols, Steroids

Straight-chain fatty alcohols (C_{14}–C_{30}), exhibited a strong predominance even over odd homologues, which resulted in CPI values that ranged from 0.01 (layers C and D) to 0.03 (layer A), but greater concentrations are observed in the upper layers A and B (20.07 and 20.42 μg/g dry mat, respectively; Table 2) The *n*-Alkanol maximum in layers A and D corresponds to *n*-18:0, whereas the most abundant homologues in layers B and C are *n*-28:0 and *n*-24:0, respectively. The content of long-chain (C_{21}–C_{30}) *n*-alkanols increases from layer A to layer C, showing the maximum in layer B. The ratio of short- to long-chain *n*-alkanols displayed a notable decrease from layer A (1.94) to the deeper layers, where comparable values (0.76–0.90) are observed (Table 2).

Branched alcohols with an isoprenoid skeleton, phytol, and isophytol are present in all layers, with concentrations varying from 0.01 to 2.22 μg/g dry mat and from 0.03 to 2.53 μg/g dry mat. The content of both compounds is the lowest in layer D and the highest in layer B (Table 2), which has the highest amount of phytane.

The C_{27}–C_{29} sterols, exhibiting the prevalence of C_{29} homologue, are present in all samples, with the highest concentration (21.27 and 26.07 μg/g dry mat) in layers B and C (Table 2). These sterols, however, are not specific to cyanobacteria, and their occurrence in the mat layers could be contributed by other eukaryotic aquatic microorganisms and higher plants. Unsaturated sterols, with a maximum at C_{29} 24-ethylcholest-5-en-3β-ol, prevail over saturated stanols in the cyanobacterial mat layer A, whereas in deeper layers, B and C the opposite trend is observed, with a maximum at 5α(H)-24-ethylcholestan-3β-ol (Table 2).

Pentacyclic triterpenoid alcohols, bishomohopanol (0.12–6.06 μg/g dry mat) and tetrahymanol (0.02–2.72 μg/g dry mat) are observed in all layers (Table 2). The concentrations of both bishomohopanol and tetrahymanol are higher in layers B and C than in layer A, and particularly layer D. Bishomohopanol is probably derived from microbial degradation of the bacteriohopanetetrols (BHPs) of cyanobacteria. Tetrahymanol has been found in sediments from a variety of depositional environments, as well as in microbial mats (Venkatesan 1989), but a higher concentration of this compound usually typifies the interface between oxic and anoxic zones in stratified water columns (Sinninghe Damsté et al. 1995).

Glycolipids and Phospholipids

The bound fatty acids (FAs) from saponification of the glycolipids (GLs) and phospholipids (PLs) fractions are typically inferred to derive from the hydrolysis of 1,2-diacylglycoglycerolipids and 1,2-diacylglycerophospholipids, respectively. FAMEs are derived from alkaline methanolysis of intact polar lipids of the PLs and GLs fractions. Both individual FAMEs and their characteristic distributions can be useful biomarkers for diverse groups of organisms in environmental samples (Allen et al. 2010).

Mass chromatograms (*m/z* 74) of methanolysis products of GLs and PLs fractions are presented in Figures 5 and 6, respectively. Mass chromatograms indicate that methanolysis products of GLs and PLs fractions obtained from the same mat are not similar in composition. FAMEs from GLs fractions showed the presence of saturated, branched, and monounsaturated compounds (Fig. 5), while FAMEs from PLs fractions almost all consist of *n*-16:0 and *n*-18:0 (Fig. 6).

Normal FAMEs were the most abundant in GLs fractions of all layers, with concentrations from 47.19 μg/g dry mat (layer B) to 72.30 μg/g dry mat (layer C). They are identified in a range from *n*-13:0 to *n*-18:0, with *n*-17:0 being absent. The branched acids are represented by C_{14}–C_{17} compounds, showing a maximum at *iso*-15:0 in all samples, and having the highest concentrations in layers B and D (Fig. 5; Table 3). The presence of monounsaturated FAMEs, *n*-16:1, *n*-18:1, and *n*-19:1 is also noticed in the GLs fraction of all layers. The concentration of monounsaturated FAMEs decreases with depth (Table 3).

DISCUSSION

The Capability of Polar-Lipid Composition for Distinguishing Individual Layers in Microbial Mats

Total Extractable Lipids

The notable decrease in TELs content from the layers A to D indicates that lipid synthesis is far more intense by aerobic rather than by anaerobic microorganisms. The prevalence of GLs and NLs in all layers (Fig. 3) can be indicative of the excess of the carbon source, whereas the nitrogen source limits microorganism growth (Alvarez and Steinbüchel 2002; Alvarez 2003). High amounts of GLs indicate a high contribution of photosynthetic organisms to the microbial mat. Also, the microbial community of natural environments is frequently exposed to many fluctuating conditions, such as variation in temperature. In these cases, the microorganisms may accumulate GLs as an energy source, favoring their survival in these variable conditions. The upper microbial mat layers differ from those lower down according to the NLs/GLs ratio (Fig. 3), indicating more intense synthesis and/or accumulation of NLs by aerobic than by anaerobic microorganisms.

TABLE 2.—*Compositions of straight- and isoprenoid chain alcohols, steroids, and triterpenoid alcohols in the layers of microbial mat*

Straight-chain alcohols (μg/g dry mat)	**A**	**B**	**C**	**D**
n-14:0	0.55	0.47	0.19	0.01
n-15:0	1.58	0.70	0.24	0.01
n-16:0	2.39	1.75	0.83	0.06
n-17:0	1.00	0.70	0.41	0.01
n-18:1w9	0.61	0.28	0.38	0.02
n-18:0	2.86	2.21	1.68	0.15
n-20:0	2.40	2.30	1.40	0.14
n-21:0	0.13	N.D.	N.D.	N.D.
n-22:0	1.75	1.90	1.22	0.09
n-23:0	0.12	0.14	0.04	N.D.
n-24:0	0.93	2.29	2.70	0.12
n-26:0	0.80	2.17	1.15	0.06
n-28:0	1.68	2.51	0.79	0.11
n-30:0	1.20	1.61	0.90	0.07
Total straight-chain alcohols (μg/g dry mat)	20.07	20.42	12.33	0.87
n-Alkanol maximum	*n*-18:0	*n*-28:0	*n*-24:0	*n*-18:0
Short-chain/long-chain *n*-alkanols	1.94	0.90	0.76	0.89
Branched-chain (isoprenoid) alcohols (μg/g dry mat)	**A**	**B**	**C**	**D**
Isophytol	1.03	2.53	2.15	0.03
Phytol	0.98	2.22	0.58	0.01
Total branched-chain alcohols (μg/g dry mat)	2.01	4.75	2.73	0.04
Steroids (μg/g dry mat)	**A**	**B**	**C**	**D**
5β(H)-Cholestan-3β-ol	0.13	0.61	0.16	N.D.
5β(H)-Cholestan-3α-ol	0.90	3.85	3.19	0.07
5α(H)-Cholestan-3-one	0.95	3.57	5.54	N.D.
Cholest-5-en-3β-ol	2.00	1.73	0.23	0.03
5α(H)-Cholestan-3β-ol	0.34	2.09	0.55	0.01
5β(H)-24-Methylcholestan-3α-ol	0.45	0.88	1.18	N.D.
24-Methylcholest-5-en-3β-ol	1.12	2.55	1.48	0.06
5α(H)-24-Methylcholestan-3β-ol	0.95	2.79	2.72	0.07
24-Ethylcholest-5,22(E)-dien-3β-ol	0.99	1.36	0.28	N.D.
Cycloartenol	0.55	1.98	0.13	N.D.
24-Ethylcholest-5-en-3β-ol	2.52	3.56	4.32	0.52
5α(H)-24-Ethylcholestan-3β-ol	1.22	4.67	7.03	0.09
Total steroids (μg/g dry mat)	12.12	29.64	26.81	0.85
Total sterols (μg/g dry mat)	11.17	26.07	21.27	0.85
C_{27} Sterols (%)	31.73	34.37	19.54	12.94
C_{28} Sterols (%)	23.73	25.82	25.45	15.29
C_{29} Sterols (%)	44.54	39.81	55.01	71.76
ΣC_{27}-C_{29} unsaturated sterols (%)	6.63	9.20	6.31	0.61
ΣC_{27}-C_{29} saturated stanols (%)	3.99	14.89	14.83	0.24
Triterpenoid alcohols (μg/g dry mat)	**A**	**B**	**C**	**D**
Bishomohopanol	1.75	6.06	3.66	0.12
Tetrahymanol	0.91	2.06	2.72	0.02
Total triterpenoid alcohols (μg/g dry mat)	2.66	8.12	6.38	0.14

N.D., not detected.

Neutral Lipids

The prevalence of a *n*-C_{17} *n*-alkane associated with prominent *n*-$C_{17:1}$ alkene is typical for cyanobacteria (Thiel et al. 1997), and has been reported in hypersaline, hot springs, and freshwater microbial mats (Grimalt et al. 1992; Fourcans et al. 2004; Rontani and Volkman 2005; Scherf and Rullkötter 2009). The result is in accordance with the domination of the *Microcoleus* taxon in the studied mat. Despite the prevalence of *n*-heptadecane in all layers, they can be distinguished by Carbon Preference Index (CPI), which reflects the ratio of odd/even *n*-alkanes, and the concentration of high-molecular-weight (HMW) *n*-alkanes (C_{22}–C_{31}). CPI showed values of 1.26, 5.21, 1.99, and 3.61 in layers A, B, C, and D, respectively. The highest content of HMW *n*-alkanes, associated with the highest amount of long-chain (C_{21}–C_{30}) *n*-alkanols in layer B (Table 2) can be attributed to the greater contribution of *Spirulina* (Franco et al. 2016), the presence of which is confirmed in the studied mat, as well as sulfate-reducing and heterotrophic bacteria. The highest impact of a sulfate-reducing bacteria to layer B is further supported by the highest ratio of hop-17(21)-ene and hop-22(29)-ene (Wolff et al. 1992) exhibiting the value of 1.42, 1.84, 1.22, and 0.92 for the layers A, B, C, and D, respectively. The increase in content of HMW *n*-alkanes in the deepest layer, D, may be indicative of anoxygenic phototrophic and heterotrophic bacteria, and it is consistent with the rise of C_{27} hopanoid content, particularly 17β(H)-22,29,30-trisnorhopane (Fig. 4).

The greater content of phytol in the upper layers, A and B, (Table 2) is consistent with its source from the phytyl side chain of chlorophyll *a* in phototrophic organisms, such as phytoplankton and cyanobacteria (Rontani and Volkman 2003). The highest concentration of both phytol and phytane in layer B may be indicative of the impact of purple sulfur bacteria, containing phytyl moiety in the bacteriochlorophyll *a* and *b* (Brooks et al. 1969; Powell and McKirdy 1973), the presence of which could have triggered the reddish color of this layer.

The differences are also observed related to the distribution of FFAs, with a higher content of long-chain homologues in the lower layers, C and D. The CPI, calculated based on the FFAs distribution, revealed a markedly higher contribution of even rather than odd FFAs homologues, and this increased with depth, although slightly less than the CPI calculated from *n*-alkanes, which displayed values from 0.17 (layer A) to 0.26 (layer D). The notable prevalence of C_{16} and C_{18} saturated FFAs, associated with their monounsaturated counterparts 16:1 and 18:1 confirmed the dominance of the cyanobacterial taxa (Abed et al. 2015). The predominance of C_{16}, C_{18}, and C_{19} compounds among the short-chain FFAs (C_{12}–C_{20}) was also reported in microalgae, zooplankton, and other bacteria (Gutiérrez et al. 2012), the presence of which was expected in the studied area.

The prevalence of C_{29} sterols in the C_{27}–C_{29} sterol distribution, observed in all layers (Table 2), is usually attributed to the impact of higher plants or brown and green algae. However, the contribution of higher plants to the studied mat is negligible, and the domination of C_{29} sterols can be related to the impact of brown and green algae. The C_{27}–C_{29} sterol distribution showed a decreasing trend in the order $C_{29} > C_{27} > C_{28}$ in the upper layers, A and B, and $C_{29} > C_{28} > C_{27}$ in the lower layers, C and D (Table 2). The higher content of C_{27} homologue in layers A and B can be attributed to the higher contribution of photosynthetic red algae in the upper layers.

The layers are also distinguished in accordance with the abundance of unsaturated sterols, and saturated stanols. The higher proportion of stanols in layers B and C compared to layers A and D (layer D contains a very low concentration of steroids due to the low impact of photosynthetic eukaryotic algae) can be evidence of the preferential degradation of sterols, which are less resistant to degradation than stanols and/or microbially mediated sterol to stanol conversion (Boudou et al. 1987). This observation agrees with the higher abundance of 5α(H)-cholestan-3-one in layers B and C than in layer A (Table 2), which is a known intermediary in the sterol → stanol conversion in algal mats. The more intense microbial activity in layers B and C is consistent with the considerably higher amount of hopanols (Table 1) in these two layers.

The highest content of bishomohopanol in layer B could be due to the higher impact of sulfate-reducing bacteria, a consideration also based on

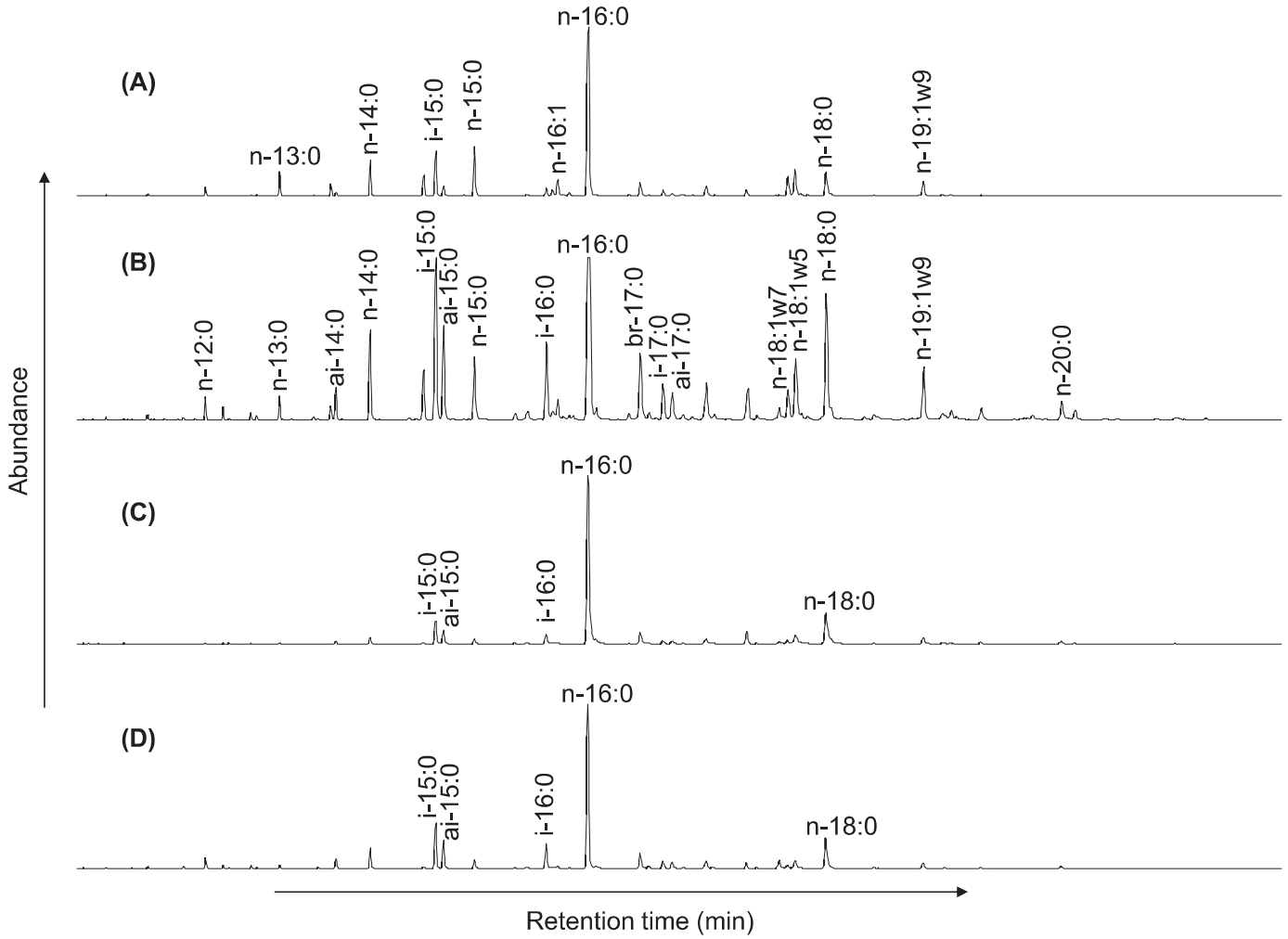

FIG. 5.—Partial mass chromatograms of *m/z* 74 showing FAMEs profiles from GLs fractions showing the presence of saturated, branched, and monounsaturated, compounds in all layers. Fatty acids are denoted as x:y, with x indicating number of carbon atoms and y giving the number of double bonds; structural isomers are denoted by prefixes: n, normal; i, iso; ai, anteiso; br, branched; additional methyl groups are noted with their position. A–D: layers from microbial mat sample.

the hop-17(21)-ene/hop-22(29)-ene ratio and the proportion of HMW *n*-alkanes. Furthermore, some studies have shown that *Planctomycetes*, *Geobacter* spp., and *Desulfovibrio* spp. are capable of hopanoid production (Sinninghe Damsté et al. 2004; Fischer et al. 2005; Härtner et al. 2005; Blumenberg et al. 2006, 2012). Therefore, the contribution from the anaerobic bacteria in layer B, and particularly layer C, should not be excluded. The highest content of tetrahymanol in layers B and C can be attributed to the marine ciliate species, most of which are scuticociliates, a widespread group of protozoa that feed mainly on bacteria (Harvey and McManus 1991). They usually occur at the interface between oxic and anoxic zones in stratified water columns (Sinninghe Damsté et al. 1995).

Glycolipids and Phospholipids

Hexadecanoic acid FAME was the most prominent compound in the GLs fractions of all samples, followed by *n*-18:0 FAME in the deeper layers B–D, whereas in layer A a hexadecenoic higher concentration of *n*-15:0 and *n*-14:0 FAME than *n*-18:0 ME is observed (Table 3). This result is consistent with the prevalence of *n*-16:0 free FA in all layers and the lowest abundance of *n*-18:0 free FA in the neutral lipids fraction of layer A.

Branched (*anteiso*- and *iso*-) and monounsaturated FAMEs were detected in the GLs fractions of all layers, with the predominance of branched FAMEs in the layers B–D and monounsaturated FAMEs in layer A (Fig. 5; Table 3). Branched FAs are commonly considered to be of bacterial origin, e.g., from sulfate-reducing bacteria (some of them could also be abundant in the oxic zones of the mats; Baumgartner et al. 2006) or sulfur-reducing bacteria (Kaneda 1991; Rütters et al. 2002). In contrast, the purple sulfur bacterium (*Chromatiaceae*) is the only biosynthesized straight-chain even-carbon-numbered FAs such as *n*-16:1, *n*-16:0, *n*-18:1, and *n*-18:0 (Imhoff and Bias-lmhoff 1995). Abundant *iso*-15:0 FA also can be an indication of a gram-positive community (Lechevalier 1988; Navarrete et al. 2000; Romano et al. 2008; Bühring et al. 2009), which are abundant in hypersaline environments (Caton et al. 2004; Ghozlan et al. 2006). Therefore, the obtained results suggest a higher contribution of sulfate-reducing and purple sulfur bacteria to layer B, which is also based on the highest content of HMW *n*-alkanes, hopanol and phytol (Table 2), as well as the highest hop-17(21)-ene/hop-22(29)-ene ratio in this layer.

The greatest concentrations of monounsaturated FAMEs, *n*-16:1 and *n*-18:1, in layers A and B agree with the contribution of *Microcoleus* sp. (Rütters et al. 2002; Bühring et al. 2009), which was the dominant cyanobacterium in the studied mat. The presence of w9 monoenoic FAME could be related to the aerobic desaturase pathway common to all cells, whereas the w7 FAMEs (Table 3) could be indicative of an anaerobic

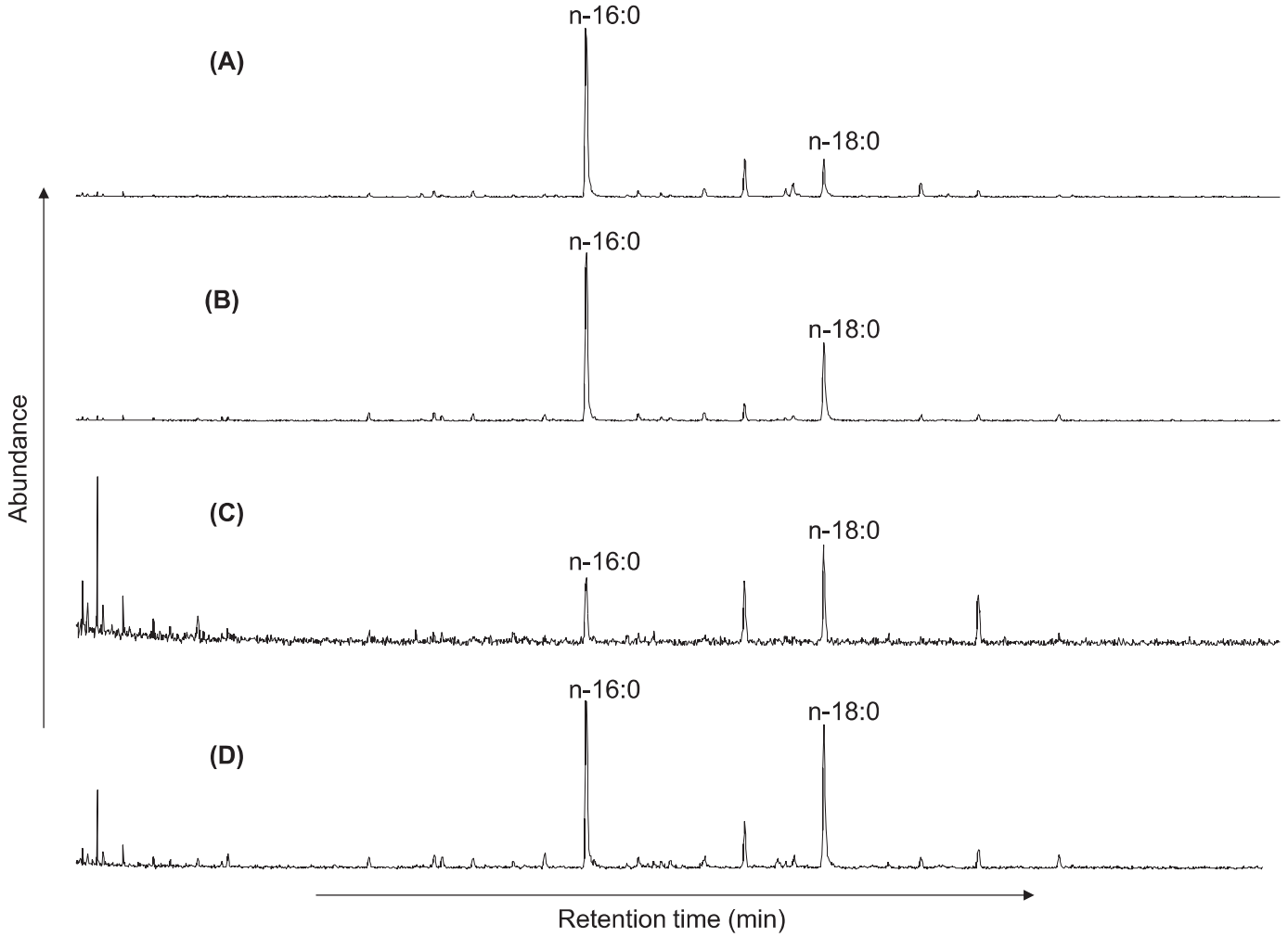

FIG. 6.—Partial mass chromatograms *of m/z* 74 showing FAMEs profiles from PLs fractions. These data show that the distribution of FAMEs in the PLs fractions of all layers is very scarce. Fatty acids are denoted as x:y, with x indicating number of carbon atoms and y giving the number of double bonds. A–D: layers from microbial mat sample.

desaturase pathway, which is often a prokaryotic biochemical pathway (Edlund et al. 1985). The higher w9/w7 ratio in layers B and C than in layer A (Table 3) is consistent with the higher concentration of eukaryotic sterols in these two layers (Table 2).

The distribution of FAMEs in the PLs fractions of all layers is very scarce (Fig. 6). This could be explained by the fact that phospholipids are quickly degraded, ranging from minutes to a few hours after cell death (Sato and Murata 1988), which is also generally reflected through the uniform low contribution of the PLs fraction (ca. 5 %; Fig. 3) to all layers.

According to Bowman et al. (1995), Hanson and Hanson (1996), and Boschker et al. (1998) the signature of phospholipid fatty acids can be used to distinguish type I mesophilic methane-oxidizing bacteria, which predominantly contain a series of *n*-16:1 mono-unsaturated PLFAs, from type II, which contain *n*-18:1 mono-unsaturated PLFAs. However, these compounds were not detected. Therefore, the predominance of *n*-16:0 PLFA over *n*-18:0 PLFA (Fig. 6), except in layer C, could be related to the contribution of the sulfate-reducing bacteria such as the *Desulfomicrobium* sp. strain.

THE RELATION OF PRECURSOR LIPIDS FROM MICROBIAL MAT TO GEOLOGIC BIOSIGNATURES

n-*Alkanes and Isoprenoid Aliphatic Alkanes*

The prevalence of short- over long-chain *n*-alkanes in source-rock extracts and petroleum, usually expressed via the TAR ratio (TAR = (n-C_{27} + n-C_{29} + n-C_{31})/(n-C_{15} + n-C_{17} + n-C_{19}); Bourbonniere and Meyers 1996) is related to the predominant aquatic source and/or high maturity of the OM. However, the high content of long-chain homologues alkanes (C_{25}–C_{33}), particularly with odd-number carbons, indicates the contribution of epicuticular waxes from land plants. As shown here, cyanobacteria synthesize a large amount of C_{17} *n*-alkane and $C_{17:1}$ *n*-alkene, which, with hydrogenation during burial, would result in the formation of C_{17} *n*-alkane. Furthermore, the distributions of free- and fatty acids bound in glyco- and phospholipids of the microbial mat sampled are characterized by a sharp prevalence of C_{16} and C_{18} homologues (Figs. 5, 6; Table 3), whereas C_{16} and C_{18} are the most abundant *n*-alkanols in all layers with the exception of layer B (Table 2). These lipids with a normal hydrocarbon skeleton produce *n*-alkanes during burial via defunctionalization. Fatty acids undergo decarboxylation, which results in the formation of *n*-alkanes

TABLE 3.—*FAMEs composition from glycolipid fractions of microbial mat.*

FAMEs from GLs (µg/g dry weight mat)				
Normal saturated	**A**	**B**	**C**	**D**
n-13:0	3.27	1.04	N.D.	0.54
n-14:0	5.66	6.00	1.69	4.66
n-15:0	8.76	4.6	1.59	2.20
n-16:0	43.17	24.73	54.90	44.16
n-18:0	5.30	10.82	14.12	9.68
Total	66.16	47.19	72.30	61.24
Branched	**A**	**B**	**C**	**D**
iso-14:0	1.68	0.77	N.D.	N.D.
anteiso-14:0	0.47	1.75	N.D.	1.99
iso-15:0	7.72	13.56	6.14	10.88
anteiso-15:0	1.62	6.69	3.28	6.29
iso-16:0	1.32	6.42	3.48	6.59
br-17:0	2.53	5.04	4.71	4.05
iso-17:0	1.03	2.58	1.42	2.13
anteiso-17:0	0.51	1.71	1.66	1.7
Total	16.88	38.52	20.69	33.63
Monounsaturated	**A**	**B**	**C**	**D**
16:1*	0.79	0.28	N.D.	N.D.
16:1w7	3.01	1.18	N.D.	N.D.
18:1w7	4.29	2.42	1.03	0.83
18:1w5	5.77	5.89	3.46	2.64
19:1w9	3.10	4.52	2.52	1.66
Total	16.96	14.29	7.01	5.13
19:1w9/(16:1w7+18:1w7)	0.42	1.26	2.45	2.00
19:1w9/18:1w7	0.72	1.87	2.45	2.00

n, normal saturated; *iso*, iso-branching; *anteiso*, anteiso-branching; br, branched at unknown position; *, Unknown position of the double bond; N.D., not detected.

having one carbon atom less; in such a case C_{16} and C_{18} fatty acids will produce C_{15} and C_{17} *n*-alkanes. Another mechanism, favored in a reducing environment, involves the reduction of FA to *n*-alcohol, dehydration to *n*-alkene, and further hydrogenation to *n*-alkane, having the same number of carbon atoms as the initial fatty acid. In this case C_{16} and C_{18} fatty acids will produce C_{16} and C_{18} *n*-alkanes. The *n*-alkanol reactions in the sedimentary record also depends on redox settings. In an oxygenated environment they undergo oxidation to fatty acids, which, with further decarboxylation, results in the formation of *n*-alkane with one carbon atom less, whereas in a reducing environment *n*-alkanols dehydrated to *n*-alkene and further hydrogenated into *n*-alkane, without a change in the number of carbon atoms. Nevertheless, regarding the redox settings, the results obtained in this study reveal that the source-rocks extracts, and petroleum derived from this microbial mat should be dominated by short-chain *n*-alkanes, with the significant prevalence of C_{15}–C_{18} homologues. Furthermore, the distribution of C_{15}–C_{18} homologues along with some other biomarker parameters (e.g., the pristane/phytane ratio, distribution of C_{31}–C_{35} homohopanes, and an abundance of gammacerane and β-carotane, see later) can be indicative of redox settings. For example, the prevalence of C_{15} and C_{17} over C_{16} and C_{18} *n*-alkanes can be indicative of a more oxidizing environment, whereas the prevalence of C_{16} and C_{18} implies reducing settings. Additionally, the distribution of mid- and long-chain *n*-alkanes (C_{22}–C_{30}) in ancient samples can contribute to determine redox depositional settings. For example, since C_{22}–C_{30} *n*-alkanols are also present in the studied mat, the prevalence of even *n*-alkane homologues in the range C_{22}–C_{30} in sedimentary OM would suggest a reducing environment, whereas the prevalence of odd *n*-alkanes would characterize oxidizing settings. These results, obtained in this study, are in agreement with literature data that petroleum derived from carbonate source rocks, in a reducing environment, are characterized by the prevalence of even *n*-alkane homologues in the range C_{22}–C_{32}, resulting in CPI < 1 (Peters et al. 2005 and references therein).

As has been already mentioned, the higher content of long-chain, particularly odd *n*-alkane homologues is usually related to the contribution of higher plants, or certain non-marine algae (e.g., *Botryococcus braunii rice A*), which may contribute to the C_{27}–C_{31} *n*-alkanes (Moldowan et al. 1985; Derenne et al. 1988). However, since the highest content of HMW *n*-alkanes (C_{22}–C_{31}) was observed in layer B, which is associated with a greater contribution of *Spirulina* (Franco et al. 2016), and sulfate-reducing and heterotrophic bacteria, the elevated content of mid- and long-chain *n*-alkanes in source-rocks extracts and petroleum derived from carbonate sources may indicate the mentioned bacterial sources. Furthermore, the increase in content of HMW *n*-alkanes in the deepest layer, D, may be indicative of anoxygenic phototrophic and heterotrophic bacteria.

Regular isoprenoids pristane (Pr) and phytane (Ph) are abundant components of source-rock extracts and petroleum. The main precursor of both components is the phytyl side chain of chlorophyll *a* in phototrophic organisms and bacteriochlorophyll *a* and *b* in purple sulfur bacteria (e.g., Brooks et al. 1969; Powell and McKirdy 1973). The formation of phytane is favored in reducing conditions, whereas the formation of pristane is related to an oxic environment. Although phytol was present in all layers of the mat, only phytane was detected in the studied samples, and no pristane was observed. The result obtained is consistent with data from the geological record, that high Pr/Ph (> 3.0) indicates input of terrigenous organic matter under oxic conditions, while low values (< 0.8) typify anoxic, commonly hypersaline or carbonate environments (Peters et al. 2005).

The presence of β-carotane in source rocks extracts and crude oils has been well documented (Philp et al. 1992; Koopmans et al. 1997; Chen et al. 2003; Hopmans et al. 2005). However, high concentrations of this biomarker are typical for anoxic lacustrine, or highly restricted marine environments (Jiang and Fowler 1986; Fu et al. 1990). The identification of β-carotane in layers A and B is consistent with the production of its precursors by cyanobacteria in arid and hypersaline environments (Jiang and Fowler 1986; Koopmans et al. 1997), whereas the absence of β-carotane in layers C and D unambiguously confirmed the fast degradation of the carotenoid skeleton by heterotrophic bacteria, and its synthesis by aerobic organisms.

Pentacyclic Triterpenoids (Hopanes and Gammacerane)

22,29,30-Trisnorhop-17(21)-ene, 17β(H)-22,29,30-trisnorhopane, hop-17(21)-ene, hop-22(29)-ene (diploptene), and bishomohopanol, detected in the studied sample, are precursors of C_{27}, C_{30}, and C_{32} hopanes, widespread in source-rock extracts and petroleum. Hopanes with 30 carbon atoms generally dominate in ancient samples, and such a pattern is also evident in the mat precursor OM (Fig. 4). The scarce distribution of hopanoids in the microbial mat in comparison with ancient sedimentary OM, where they are usually present in the C_{27}–C_{35} range, is related to the fact that hopanoids are generally bounded into macromolecules via a larger number of binding sites (particularly the numerous hydroxyl groups) other than other biomarkers (Hofmann et al. 1991; Richnow et al. 1991; Rohmer 1993). This may lead to their preferential incorporation into macromolecules, during early diagenesis, and their retention in the bound fractions up to cracking in the oil-window stage (Hofmann et al. 1991; Bowden et al. 2006). On the other hand, C_{30} hop-17(21)-ene, C_{30} hop-22(29)-ene, C_{27} 22,29,30-trisnorhop-17(21)-ene, and C_{27} 17β(H)-22,29,30-trisnorhopane do not have hydroxyl groups and consequently remained free or have been weakly adsorbed by the OM and therefore has been easily detected in the microbial mat. Our assumption is confirmed by the presence of a full series of hopanoids typical for the geological record observed in the liquid

products obtained by hydrous pyrolysis of the studied microbial mat (Franco et al. 2016).

Tetrahymanol, detected in all layers (Table 2), is the main precursor of gammacerane in source rocks and petroleum. Although present at least in trace amounts in most source-rock extracts and petroleum, a large amount of gammacerane is generally related to highly reducing, hypersaline conditions during the deposition of the OM (Moldowan et al. 1985; Fu et al. 1986), which also coincides with our results, particularly from layers B and C. Moreover, the high content of gammacerane in carbonate-derived source rocks and petroleum is usually associated with the elevated content of phytane (e.g., low pristane/phytane ratio), and the precursors of both compounds (tetrahymanol and phytol; Table 2), as well as phytane were identified in all layers, whereas pristane was absent.

Steroids

The distribution of 5α(H)14α(H)17α(H)20(*R*) C_{27}–C_{29} regular steranes is a routine parameter used in the evaluation of the sedimentary OM type. It is based on the observation that C_{27} steranes originate dominantly from marine plankton and red algae (Huang and Meinschein 1979; Schwark and Empt 2006), C_{28} steranes from yeast, fungi, plankton and algae (Volkman 2003), and C_{29} homologues from higher plants (Volkman 1986), and brown and green algae (Volkman 2003). Marine environments are generally characterized by the prevalence of C_{27} or C_{29} sterane homologues, which is in agreement with the distribution of precursor C_{27}–C_{29} sterols observed in the studied mat, since the conversion of sterols into steranes during geothermal maturation does not change the total number of carbon atoms in the molecule.

CONCLUSIONS

The studied hypersaline mat has a flat dark pigmented green surface and internally was subdivided into four colored layers (A–D). The top of the mat had a green layer, A (0.5 cm), followed by a reddish-brown layer, B (0.5–1.5 cm), a dark brown greenish (1.5–3.0 cm) layer, C, and a thicker bottom brown layer, D (3.0–6.0 cm). Cyanobacterial taxa dominate the biomass with a diversity of the 16 morphospecies in which *Microcoleus chthonoplastes* prevails. Based on the studied lipid classes the contribution of sulfate-reducing bacteria such as *Desulfomicrobium* sp. strain, purple sulfur bacteria, as well as the possible input of *Geobacter* spp. and *Desulfovibrio* spp., particularly in the deeper layers, is also established.

A notable decrease in the total extractable lipid yield from layers A to D indicates that lipid synthesis is far more intense by the photosynthesizing cyanobacteria than by anaerobic microorganisms. The content of PLs was uniform and very low (< 5%) in all layers, confirming an extremely quick degradation (from minutes to a few hours) after cell death. Therefore, the layers can be more effectively distinguished based on the composition of NLs and GLs than the composition of PLs. GLs that are accumulated as an energy source, followed by NLs, were most abundant in all layers, indicating the medium which is characterized by excess of the carbon source and limitation of microorganism growth by the nitrogen source.

The lipid composition showed an adequate capability to distinguish individual layers in the microbial mat. The NLs/GLs ratio decreases from layer A to layer D. Among the studied lipid classes, the observed layers mostly differ according to the amount of high-molecular-weight *n*-alkanes and long-chain (C_{21}–C_{30}) *n*-alkanols, the content of phytol, hopanol, and sterols, the stanol/sterol ratio, the content of branched FAs in the GLs fraction, as well as the w9/w7 FA ratio of the GLs fraction. All the mentioned parameters generally increase with depth, being commonly the highest in layer B, which implies a greater contribution of sulfate-reducing and purple sulfur bacteria to this layer. Furthermore, based on the distribution of C_{27}–C_{29} sterols a higher impact of photosynthetic red algae is suggested in the upper layers, A and B, whereas the highest content of tetrahymanol in layers B and C indicates an elevated contribution of marine ciliate species, feeding on bacteria, in these two layers. The greatest capability for hydrocarbons synthesis is observed in layer B. Our results also imply microbially mediated lipid diagenetic alteration, particularly in layers B and C.

Comparison of the composition of lipid classes in the microbial mat and distributions of the biomarkers in ancient source-rocks extracts and petroleum implies that the precursor lipids provide essential data to understand the transformation of the microbial OM during the sedimentation processes and its contribution to the fossil record. This is particularly related to the distribution of *n*-alkanes, the high abundance of phytane and gammacerane, as well as the distribution of C_{27}–C_{29} regular steranes in source rocks and petroleum derived from carbonate hypersaline environments. The sole limitation in the direct connection of the lipid composition in the microbial mats and the fossil biomarkers concerns the distribution of hopanes due to the fact that hopanoids are preferentially bounded into macromolecules, during very early diagenesis, and their more intense release occurs by cracking in the early oil-window stage. This could explain why hopanes (C_{31}–C_{35}), usually found in rock extracts and oils, are missing in the studied mat. Furthermore, the chemical composition of the mat species and the biogeochemical process occurring in the mats vary in response to changes in the salinity, water cover, light intensity, and temperature in the microbial-mat setting. Finally, it would be worth testing whether these factors are changing the microbial biosignatures. Respective results could help to better identify microbial biomarkers in the geological record.

ACKNOWLEDGMENTS

The authors are grateful to PETROBRAS-Brazil, Coordenação de Aperfeioamento de Pessoal de Nível Superior (CAPES), Conselho Nacional de Desenvolvimento Científico e Tecnológico (CNPq), and Fundação de Amparo à Pesquisa do Estado do Rio de Janeiro (FAPERJ). We thank Peter Burgess, Cody Miller, Gene Rankey, and John Southard for constructive reviews and comments, which significantly improved the manuscript.

REFERENCES

Abed, R.M.M., and Garcia-Pichel, F., 2001, Long-term compositional changes after transplant in a microbial mat cyanobacterial community revealed using a polyphasic approach: Environmental Microbiology, v. 3, p. 53–62.

Abed, R.M.M., Kohls, K., Schoon, R., Scherf, A.-K., Schacht, M., Palinska, K.A., Al-Hassani, H., Hamza, W., Rullkötter, J., and Golubic, S., 2008, Lipid biomarkers, pigments and cyanobacterial diversity of microbial mats across intertidal flats of the arid coast of the Arabian Gulf (Abu Dhabi, UAE): FEMS Microbiology Ecology, v. 65, p. 449–462.

Abed, R.M.M., Klempová, T., Gajdoš, P., and Čertík, M., 2015, Bacterial diversity and fatty acid composition of hypersaline cyanobacterial mats from an inland desert wadi: Journal of Arid Environments, v. 115, p. 81–89.

Allen, M.A., Neilan, B.A., Burns, B.P., Jahnke, L.L., and Summons, R.E., 2010, Lipid biomarkers in Hamelin Pool microbial mats and stromatolites: Organic Geochemistry, v. 41, p. 1207–1218.

Alvarez, H.M., 2003, Relationship between β-oxidation pathway and the hydrocarbon-degrading profile in actinomycetes bacteria: International Biodeterioration & Biodegradation, v. 52, p. 35–42.

Alvarez, H., and Steinbüchel, A., 2002, Triacylglycerols in prokaryotic microorganisms: Applied Microbiology and Biotechnology, v. 60, p. 367–376.

Banerjee, A., Sharma, R., Chisti, Y., and Banerjee, U.C., 2002, *Botryococcus braunii*: a renewable source of hydrocarbons and other chemicals: Critical Reviews in Biotechnology, v. 22, p. 245–279.

Baumgartner, L.K., Reid, R.P., Dupraz, C., Decho, A.W., Buckley, D.H., Spear, J.R., Przekop, K.M., and Visscher, P.T., 2006, Sulfate reducing bacteria in microbial mats: changing paradigms, new discoveries: Sedimentary Geology, v. 185, p. 131–145.

Blumenberg, M., Krüger, M., Nauhaus, K., Talbot, H.M., Oppermann, B.I., Seifert, R., Pape, T., and Michaelis, W., 2006, Biosynthesis of hopanoids by sulfate-reducing bacteria (genus *Desulfovibrio*): Environmental Microbiology, v. 8, p. 1220–1227.

Blumenberg, M., Thiel, V., Riegel, W., Kah, L.C., and Reitner, J., 2012, Biomarkers of black shales formed by microbial mats, late Mesoproterozoic (1.1 Ga) Taoudeni Basin, Mauritania: Precambrian Research, v. 196–197, p. 113–127.

Boschker, H.T.S., Nold, S.C., Wellsbury, P., Bos, D., de Graaf, W., Pel, R., Parkes, R.J., and Cappenberg, T.E., 1998, Direct linking of microbial populations to specific biogeochemical processes by ^{13}C-labeling of biomarkers: Nature, v. 392, p. 801–805.

Boudou, J.P., Trichet, J., Robinson, N., and Brassell, S.C., 1986, Lipid composition of a Recent Polynesian microbial mat sequence: Organic Geochemistry, v. 10, p. 705–709.

Boudou, J.P., Boulégue, J., Maléchaux, L., Nip, M., de Leeuw, J.W., and Boon, J.J., 1987, Identification of some sulphur species in a high organic sulphur coal: Fuel, v. 66, p. 1558–1569.

Bourbonniere, R.A., and Meyers, P.A., 1996, Sedimentary geolipid records of historical changes in the watersheds and productivities of lakes Ontario and Erie: Limnology and Oceanography, v. 41, p. 352–359.

Bowden, S.A., Farrimond, P., Snape, C.E., and Love, G.D., 2006, Compositional differences in biomarker constituents of the hydrocarbon, resin, asphaltene and kerogen fractions: an example from the Jet Rock (Yorkshire, UK): Organic Geochemistry, v. 37, p. 369–383.

Bowman, J.P., Sly, L.I., and Stackebrandt, E., 1995, The phylogenetic position of the Family Methylococcaceae: International Journal of Systematic and Evolutionary Microbiology, v. 45, p. 182–185.

Brooks, J.D., Gould, K., and Smith, J.W., 1969, Isoprenoid hydrocarbons in coal and petroleum: Nature, v. 222, p. 257–259.

Bühring, S.I., Smittenberg, R.H., Sachse, D., Lipp, J.S., Golubic, S., Sachs, J.P., Hinrichs, K.-U., and Summons, R.E., 2009, A hypersaline microbial mat from the Pacific Atoll Kiritimati: insights into composition and carbon fixation using biomarker analyses and a ^{13}C-labeling approach: Geobiology, v. 7, p. 308–323.

Caton, T.M., Witte, L.R., Ngyuen, H.D., Buchheim, J.A., Buchheim, M.A., and Schneegurt, M.A., 2004, Halotolerant aerobic heterotrophic bacteria from the Great Salt Plains of Oklahoma: Microbial Ecology, v. 48, p. 449–462.

Chen, J., Liang, D., Wang, X., Zhong, N., Song, F., Deng, C., Shi, X., Jin, T., and Xiang, S., 2003, Mixed oils derived from multiple source rocks in the Cainan oilfield, Junggar Basin, northwest China. Part I: genetic potential of source rocks, features of biomarkers, and oil sources of typical crude oils: Organic Geochemistry, v. 34, p. 889–909.

Damazio, C.M., and Silva E Silva, L.H., 2006, Cianobactérias em esteiras microbianas coloformes da lagoa Pitanguinha, Rio de Janeiro, Brasil: Revista Brasileira de Paleontologia, v. 9, p. 165–170.

Derenne, S., Largeau, C., Casadevall, E., and Connan, J., 1988, Comparison of torbanites of various origins and evolutionary stages. Bacterial contribution to their formation. Cause of lack of botryococcane in bitumens: Organic Geochemistry, v. 12, p. 43–59.

Dijkman, N.A., Boschker, H.T.S., Stal, L.J., and Kromkamp, J.C., 2010, Composition and heterogeneity of the microbial community in a coastal microbial mat as revealed by the analysis of pigments and phospholipid-derived fatty acids: Journal of Sea Research, v. 63, p. 62–70.

Dobson, G., Ward, D.M., Robinson, N., and Eglinton, G., 1988, Biogeochemistry of hot spring environments: extractable lipids of a cyanobacterial mat: Chemical Geology, v. 68, p. 155–179.

Edlund, A., Nichols, P.D., Roffey, R., and White, D.C., 1985, Extractable and lipopolysaccharide fatty acid and hydroxy acid profiles from *Desulfovibrio* species: Journal of Lipid Research, v. 26, p. 982–988.

Fischer, W.W., Summons, R.E., and Pearson, A., 2005, Targeted genomic detection of biosynthetic pathways: anaerobic production of hopanoid biomarkers by a common sedimentary microbe: Geobiology, v. 3, p. 33–40.

Fourcans, A., de Oteyza, T.G., Wieland, A., Solé, A., Diestra, E., van Bleijswijk, J., Grimalt, J.O., Kuhl, M., Esteve, I., Muyzer, G., Caumette, P., and Duran, R., 2004, Characterization of functional bacterial groups in a hypersaline microbial mat community (Salins-de-Giraud, Camargue, France): FEMS Microbiology Ecology, v. 51, p. 55–70.

Franco, N., Mendonça Filho, J.G., Silva, T.F., Stojanović, K., Fontana, L.F., Carvalhal-Gomes, S.B.V., Silva, F.S., and Furukawa, G.G., 2016, Geochemical characterization of the hydrous pyrolysis products from a recent cyanobacteria-dominated microbial mat: Geologica Acta, v. 14, p. 385–401.

Fu, J., Sheng, G., Peng, P., Brassell, S., Eglinton, G., and Jigang, J., 1986, Peculiarities of salt lake sediments as potential source rocks in China: Organic Geochemistry, v. 10, p. 119–126.

Fu, J., Sheng, G., Xu, J., Eglinton, G., Gowar, A.P., Jia, R., and Fan, S., 1990, Application of biological markers in assessment of paleoenvironments of Chinese non-marine sediments: Organic Geochemistry, v. 16, p. 769–779.

Garcia-Pichel, F., Prufert-Bebout, L., and Muyzer, G., 1996, Phenotypic and phylogenetic analyses show *Microcoleus chthonoplastes* to be a cosmopolitan cyanobacterium: Applied and Environmental Microbiology, v. 62, p. 3284–3291.

Ghozlan, H., Deif, H., Kandil, R.A., and Sabry, S., 2006, Biodiversity of moderately halophilic bacteria in hypersaline habitats in Egypt: The Journal of General and Applied Microbiology, v. 52, p. 63–72.

Gillan, F.T., and Sandstrom, M.W., 1985, Microbial lipids from a nearshore sediment from Bowling Green Bay, North Queensland: the fatty acid composition of intact lipid fractions: Organic Geochemistry, v. 8, p. 321–328.

Grimalt, J.O., de Wit, R., Teixidor, P., and Albaigés, J., 1992, Lipid biogeochemistry of Phormidium and Microcoleus mats: Organic Geochemistry, v. 19, p. 509–530.

Gutiérrez, M.H., Pantoja, S., and Lange, C.B., 2012, Biogeochemical significance of fatty acid distribution in the coastal upwelling ecosystem off Concepción (36°S), Chile: Organic Geochemistry, v. 49, p. 56–67.

Hanson, R.S., and Hanson, T.E., 1996, Methanotrophic bacteria: Microbiological Reviews, v. 60, p. 439–471.

Härtner, T., Straub, K.L., and Kannenberg, E., 2005, Occurrence of hopanoid lipids in anaerobic Geobacter species: FEMS Microbiology Letters, v. 243, p. 59–64.

Harvey, H.R., and McManus, G.B., 1991, Marine ciliates as a widespread source of tetrahymanol and hopan-3β-ol in sediments: Geochimica et Cosmochimica Acta, v. 55, p. 3387–3390.

Hofmann, I.C., Hutchinson, J., Robson, J.N., Chicarelli, M.I., and Maxwell, J.R., 1991, Evidence for sulphide links in a crude oil asphaltene and kerogens from reductive cleavage by lithium in ethylamine: Organic Geochemistry, v. 19, p. 371–387.

Hopmans, E.C., Schouten, S., Rijpstra, W.I.C., and Sinninghe Damsté, J.S., 2005, Identification of carotenals in sediments: Organic Geochemistry, v. 36, p. 485–495.

Horodyski, R.J., and Bloeser, B., 1977, Laminated algal mats from a coastal lagoon, Laguna Mormona, Baja California, Mexico: Journal of Sedimentary Research, v. 47, p. 680–696.

Huang, W.-Y., and Meinschein, W.G., 1979, Sterols as ecological indicators: Geochimica et Cosmochimica Acta, v. 43, p. 739–745.

Imhoff, J.F., and Bias-lmhoff, U. 1995, Lipids, quinones and fatty acids of anoxygenic phototrophic bacteria, *in* Blankenship, R.E., Madigan, M.T., and Bauer, C.E., eds., Anoxygenic Photosynthetic Bacteria: Dordrecht, Springer, p. 179–205.

Jiang, Z.S., and Fowler, M.G., 1986, Carotenoid-derived alkanes in oils from northwestern China: Organic Geochemistry, v. 10, p. 831–839.

Jonkers, H.M., Ludwig, R., De Wit, R., Pringault, O., Muyzer, G., Niemann, H., Finke, N., and De Beer, D., 2003, Structural and functional analysis of a microbial mat ecosystem from a unique permanent hypersaline inland lake: "La Salada de Chiprana" (NE Spain): FEMS Microbiology Ecology, v. 44, p. 175–189.

Kaneda, T., 1991, Iso- and anteiso-fatty acids in bacteria: biosynthesis, function, and taxonomic significance: Microbiological Reviews, v. 55, p. 288–302.

Kates, M., 1972, Ether-linked lipids in extremely halophilic bacteria, *in* Snyder, F., ed., Ether Lipids Chemistry and Biology: Academic Press, p. 351–398.

Kaur, G., Mountain, B.W., Hopmans, E.C., and Pancost, R.D., 2011, Relationship between lipid distribution and geochemical environment within Champagne Pool, Waiotapu, New Zealand: Organic Geochemistry, v. 42, p. 1203–1215.

Knoppers, B. and Kjerfve, B., 1999, Coastal lagoons of southeastern brazil: physical and biogeochemical characteristics, *in* Perillo, G.M.E., Piccolo, M.C., and Pino-Quivira, M., eds., Estuaries of South America: Their Geomorphology and Dynamics: Berlin, Springer, p. 35–66.

Koopmans, M.P., de Leeuw, J.W., and Sinninghe Damsté, J.S., 1997, Novel cyclised and aromatised diagenetic products of β-carotene in the Green River Shale: Organic Geochemistry, v. 26, p. 451–466.

Laut, L., Martins, M.V.A., Frontalini, F., Ballalai, J.M., Belart, P., Habib, R., Fontana, L.F., Clemente, I.M.M.M., Lorini, M.L., Mendonça Filho, J.G., Laut, V.M., and Figueiredo, M., 2017, Assessment of the trophic state of a hypersaline-carbonatic environment: Vermelha Lagoon (Brazil): PLOS One, v. 12, p. e0184819.

Lechevalier, H., 1988, Chemotaxonomic use of lipids: an overview: Microbial Lipids, v. 1, p. 869–902.

Lechevalier, M.P., and Moss, C.W., 1977, Lipids in bacterial taxonomy: a taxonomist's view: Critical Reviews in Microbiology, v. 5, p. 109–210.

Lehtonen, K., and Ketola, M., 1993, Solvent-extractable lipids of Sphagnum, Carex, Bryales and Carex–Bryales peats: content and compositional features vs. peat humification: Organic Geochemistry, v. 20, p. 363–380.

Moldowan, J.M., Seifert, W.K., and Gallegos, E.J., 1985, Relationship between petroleum composition and depositional environment of petroleum source rocks: American Association of Petroleum Geologists, Bulletin, v. 69, p. 1255–1268.

Moreira, N.F., Walter, L.M., Vasconcelos, C., McKenzie, J.A., and McCall, P.J., 2004, Role of sulfide oxidation in dolomitization: sediment and pore-water geochemistry of a modern hypersaline lagoon system: Geology, v. 32, p. 701–704.

Navarrete, A., Peacock, A., MacNaughton, S.J., Urmeneta, J., Mas-Castellà, J., White, D.C., and Guerrero, R., 2000, Physiological status and community composition of microbial mats of the Ebro Delta, Spain by signature lipid biomarkers: Microbial Ecology, v. 39, p. 92–99.

Nytoft, H.P., 2011, Novel side chain methylated and hexacyclic hopanes: identification by synthesis, distribution in a worldwide set of coals and crude oils and use as markers for oxic depositional environments: Organic Geochemistry, v. 42, p. 520–539.

Ourisson, G., and Rohmer, M., 1992, Hopanoids. 2. Biohopanoids: a novel class of bacterial lipids: Accounts of Chemical Research, v. 25, p. 403–408.

Pagès, A., Grice, K., Ertefai, T., Skrzypek, G., Jahnert, R., and Greenwood, P., 2014, Organic geochemical studies of modern microbial mats from Shark Bay: Part I: influence of depth and salinity on lipid biomarkers and their isotopic signatures: Geobiology v. 12, p. 469–487.

Peters, K.E., Walters, C.C., and Moldowan, J.M., 2005, The Biomarker Guide, Volume 2: Biomarkers and Isotopes in the Petroleum Exploration and Earth History: Cambridge, UK, Cambridge University Press, 680 p.

Philp, R.P., Chen, J.H., Fu, J.M., and Sheng, G.Y., 1992, A geochemical investigation of crude oils and source rocks from Biyang Basin, China: Organic Geochemistry, v. 18, p. 933–945.

Pierson, B.K., Valdez, D., Larsen, M., Morgan, E., and Mack, E.E., 1994, Chloroflexus-like organisms from marine and hypersaline environments: distribution and diversity: Photosynthesis Research, v. 41, p. 35–52.

Piorreck, M., and Pohl, P., 1984, Formation of biomass, total protein, chlorophylls, lipids and fatty acids in green and blue-green algae during one growth phase: Phytochemistry, v. 23, p. 217–223.

Plet, C., Pagès, A., Holman, A.I., Madden, R.H.C., and Grice, K., 2018, From supratidal to subtidal, an integrated characterisation of Carbla Beach shallow microbial mats (Hamelin Pool, Shark Bay, WA): lipid biomarkers, stable carbon isotopes and microfabrics: Chemical Geology, v. 493, p. 338–352.

Powell, T.G., and McKirdy, D.M., 1973, Relationship between ratio of pristane to phytane, crude oil composition and geological environment in Australia: Nature, v. 243, p. 37–39.

Ramos, V.M.C., Castelo-Branco, R., Leão, P.N., Martins, J., Carvalhal-Gomes, S., Sobrinho da Silva, F., Mendonça Filho, J.G., and Vasconcelos, V.M., 2017, Cyanobacterial diversity in microbial mats from the hypersaline lagoon system of Araruama, Brazil: an in-depth polyphasic study: Frontiers in Microbiology, v. 8, p. 1233.

Řezanka, T., Sokolov, M.Y., and Víden, I., 1990, Unusual and very-long-chain fatty acids in *Desulfotomaculum*, a sulfate-reducing bacterium: FEMS Microbiology Ecology, v. 6, p. 231–237.

Řezanka, T., Zlatkin, I.V., Víden, I., Slabova, O.I., and Nikitin, D.I., 1991, Capillary gas chromatography-mass spectrometry of unusual and very long-chain fatty acids from soil oligotrophic bacteria: Journal of Chromatography A, v. 558, p. 215–221.

Richert, L., Golubic, S., Le Guédès, R., Hervé, A., and Payri, C., 2006, Cyanobacterial populations that build "kopara" microbial mats in Rangiroa, Tuamotu Archipelago, French Polynesia: European Journal of Phycology, v. 41, p. 259–279.

Richnow, H.H., Jenisch, A., and Michaelis, W., 1991, Structural investigations of sulphur-rich macromolecular oil fractions and a kerogen by sequential chemical degradation: Organic Geochemistry, v. 19, p. 351–370.

Riding, R., 2000, Microbial carbonates: the geological record of calcified bacterial–algal mats and biofilms: Sedimentology, v. 47, p. 179–214.

Rocha, L., and Borgui, L., 2017, Análise de microbiofácies das esteiras microbianas da Lagoa Pitanguinha (Região dos Lagos, RJ, Brasil): Anuário do Instituto de Geociências, v. 40, p. 191–205.

Rohmer, M., 1993, The biosynthesis of triterpenoids of the hopane series in the Eubacteria: a mine of new enzyme reactions: Pure and Applied Chemistry, v. 65, p. 1293–1298.

Rohmer, M., Bouvier-Nave, P., and Ourisson, G., 1984, Distribution of hopanoid triterpenes in prokaryotes: Microbiology, v. 130, p. 1137–1150.

Romano, I., Finore, I., Nicolaus, G., Huertas, F.J., Lama, L., Nicolaus, B., and Poli, A., 2008, *Halobacillus alkaliphilus* sp. nov., a halophilic bacterium isolated from a salt lake in Fuente de Piedra, southern Spain: International Journal of Systematic and Evolutionary Microbiology, v. 58, p. 886–890.

Rontani, J.-F., and Volkman, J.K., 2003, Phytol degradation products as biogeochemical tracers in aquatic environments: Organic Geochemistry, v. 34, p. 1–35.

Rontani, J.-F., and Volkman, J.K., 2005, Lipid characterization of coastal hypersaline cyanobacterial mats from the Camargue (France): Organic Geochemistry, v. 36, p. 251–272.

Rütters, H., Sass, H., Cypionka, H., and Rullkötter, J., 2002, Phospholipid analysis as a tool to study complex microbial communities in marine sediments: Journal of Microbiological Methods, v. 48, p. 149–160.

Sánchez, O., Ferrera, I., Vigués, N., Oteyza, T.G., Grimalt, J., and Mas, J., 2006, Role of cyanobacteria in oil biodegradation by microbial mats: International Biodeterioration & Biodegradation, v. 58, p. 186–195.

Saïto, N., and Murata, N., 1988, Membrane lipids: Methods in Enzymology, v. 167, p. 251–259.

Scherf, A.-K., and Rullkötter, J., 2009, Biogeochemistry of high salinity microbial mats: Part 1: lipid composition of microbial mats across intertidal flats of Abu Dhabi, United Arab Emirates: Organic Geochemistry, v. 40, p. 1018–1028.

Schwark, L., and Empt, P., 2006, Sterane biomarkers as indicator of palaeozoic algal evolution and extinction events: Palaeogeography, Palaeoclimatology, Palaeoecology, v. 240, p. 225–236.

Silva E Silva, L.H., and Carvalhal, S.B.V., 2005, Biolaminóides calcários Holocênicos da Lagoa Vermelha, Brasil: Anuário do Instituto de Geociências, v. 28, p. 59–70.

Silva E Silva, L.H., Senra, M.C.E., Faruolo, T.C.L.M., Carvalhal, S.B.V., Alves, S.A.P.M.N., Damazio, C.M., Shimizu, V.T.A., Santos, R.C., and Iespa, A.A.C., 2004, Composição paleobiológica e tipos morfológicos das construções estromatolíticas da Lagoa Vermelha, RJ, Brasil: Revista Brasileira de Paleontologia, v. 7, p. 193–198.

Silva E Silva, L.H., Damazio, C.M., and Iespa, A.A.C., 2005, Registro de biolaminóides poligonais na Lagoa de Araruama, Estado do Rio de Janeiro, Brasil: Revista de Geologia, v. 18, p. 153–158.

Sinninghe Damsté, J.S., Kenig, F., Koopmans, M.P., Köster, J., Schouten, S., Hayes, J.M., and de Leeuw, J.W., 1995, Evidence for gammacerane as an indicator of water column stratification: Geochimica et Cosmochimica Acta, v. 59, p. 1895–1900.

Sinninghe Damsté, J.S., Rijpstra, W.I.C., Schouten, S., Fuerst, J.A., Jetten, M.S.M., and Strous, M., 2004, The occurrence of hopanoids in planctomycetes: implications for the sedimentary biomarker record: Organic Geochemistry, v. 35, p. 561–566.

Stolz, J.F., 2000, Structure of microbial mats and biofilms, *in* Riding, R.E., and Awramik, S.M., eds., Microbial Sediments: Berlin, Springer-Verlag, p. 1–8.

Summons, R.E., Jahnke, L.L., and Roksandic, Z., 1994, Carbon isotopic fractionation in lipids from methanotrophic bacteria: relevance for interpretation of the geochemical record of biomarkers: Geochimica et Cosmochimica Acta, v. 58, p. 2853–2863.

Thiel, V., Merz-Preiß, M., Reitner, J., and Michaelis, W., 1997, Biomarker studies on microbial carbonates: extractable lipids of a calcifying cyanobacterial mat (Everglades, USA): Facies, v. 36, p. 163–172.

Tissot, B.P., and Welte, D.H., 1984, Petroleum Formation and Occurrence, 2nd Edition: Heidelberg, Springer-Verlag, 669 p.

van Gemerden, H., 1993, Microbial mats: a joint venture: Marine Geology, v. 113, p. 3–25.

van Lith, Y., Vasconcelos, C., Warthmann, R., Martins, J.C.F., and McKenzie, J.A., 2002, Bacterial sulfate reduction and salinity: two controls on dolomite precipitation in Lagoa Vermelha and Brejo do Espinho (Brazil): Hydrobiologia, v. 485, p. 35–49.

Vasconcelos, C., Warthmann, R., McKenzie, J.A., Visscher, P.T., Bittermann, A.G., and van Lith, Y., 2006, Lithifying microbial mats in Lagoa Vermelha, Brazil: Modern Precambrian relics?: Sedimentary Geology, v. 185, p. 175–183.

Venkatesan, M.I., 1988, Diploptene in Antarctic sediments: Geochimica et Cosmochimica Acta, v. 52, p. 217–222.

Venkatesan, M.I., 1989, Tetrahymanol: its widespread occurrence and geochemical significance: Geochimica et Cosmochimica Acta, v. 53, p. 3095–3101.

Visscher, P.T., Prins, R.A., and van Gemerden, H., 1992, Rates of sulfate reduction and thiosulfate consumption in a marine microbial mat: FEMS Microbiology Ecology, v. 9, p. 283–293.

Volkman, J.K., 1986, A review of sterol markers for marine and terrigenous organic matter: Organic Geochemistry, v. 9, p. 83–99.

Volkman, J.K., 2003, Sterols in microorganisms: Applied Microbiology and Biotechnology, v. 60, p. 496–506.

Volkman, J.K., Allen, D.I., Stevenson, P.L., and Burton, H.R., 1986, Bacterial and algal hydrocarbons in sediments from a saline Antarctic lake, Ace Lake: Organic Geochemistry, v. 10, p. 671–681.

Ward, D.M., Ferris, M.J., Nold, S.C., and Bateson, M.M., 1998, A natural view of microbial biodiversity within hot spring cyanobacterial mat communities: Microbiology and Molecular Biology Reviews, v. 62, p. 1353–1370.

Wolfe, G.A., Ruskin, N., and Marshal, J.D., 1992, Biogeochemistry of an early diagenetic concretion from the Birchi Bed (L. Lias, W. Dorset, UK): Organic Geochemistry, v. 19, p. 431–444.

Received 13 August 2019; accepted 1 October 2020.